Advances in Concrete Construction, *Vol. 9, No. 3 (2020) 249-256*
DOI: https://doi.org/10.12989/acc.2020.9.3.249

Mechanical behavior of crumb rubber concrete under axial compression

Rui Ren[1,2], Jiong-Feng Liang*[3], Da-wei Liu[3], Jin-he Gao[3] and Lin Chen[3]

[1]School of Civil Engineering, Xi'an University of Architecture & Technology, Xi'an 710055, China
[2]State Key Laboratory of Green Building in Western China, Xi'an University of Architecture & Technology, Xi'an 710055, China
[3]School of Civil & Architecture Engineering, East China University of Technology, Nanchang 330013, China

(*Received January 3, 2019, Revised December 2, 2019, Accepted January 18, 2020*)

Abstract. This paper aims at investigating the effect of crumb rubber size and content on compressive behaviors of concrete under axial compression. Concrete specimens are designed and produced by replacing natural aggregate with crumb rubber content of 0%, 5%, 10%, 15% and three different sized crumb rubbers (No. 20, No. 40, No. 80 crumb rubber). And the failure mode, compressive strength, elastic modulus, stress-strain curves, peak strain and ultimate strain are experimentally studied. Based on the test results, formulas have been presented to determine the compressive strength, elastic modulus, the relationship between prism compressive strength and cube compressive strength, stress-strain curves and peak strain of crumb rubber concrete (CRC). It is found that the proposed formulas agree well with the test result on the whole, which may be used to practical applications.

Keywords: crumb rubber; concrete; stress-strain; axial compression; compressive strength

1. Introduction

In recent years, the development of automobile industry and transportation industry, it has led to a sharp increase in waste rubber as a by-product, posing tremendous pressure and challenges to the sustainable development of environment and resources. However, incorporating rubber into concrete can reduce environmental pollution and conserve resources. And, due to the low specific gravity of crumb rubber particles, the unit weight of the rubber concrete decreases as the percentage of crumb rubber replacement increases. The non polarity of crumb rubber causes water to be repelled and the air to consequently be trapped on the surface; the air content in the rubber concrete increases as the rubber content increases. This new kind of crumb rubber concrete has been studied by some researchers (Emiroglu *et al.* 2015, Thomas *et al.* 2015, Padhi and Panda 2016, Gupta *et al.* 2017). These results found that the incorporation of rubber particles into concrete results in better resilience, durability and deformation ability of the concrete.

Previous works focused on the examination of the mechanical properties and durability of crumb rubber concrete. Fu *et al.* (2019) studied the evolution of strength (compressive, tensile, and flexural) and toughness of steel fiber-reinforced rubberized concrete with various fiber dosages and rubber contents. The results showed that the compressive strength of steel fiber-reinforced rubberized concrete was dependent on both rubber content and fiber dosage, while the flexural and tensile strengths were dominated by the fiber dosage. Ramdani *et al.* (2019) studied the effect of incorporating waste rubber aggregates in combination with waste glass powder or silica sand powder obtained from dune natural sand, on the performances of cementitious mixtures. The results showed that the strength increased with the incorporation of glass powder and rubber aggregates, especially with 10% and 20% rubber aggregates contents. Zhang and Poon (2018) developed an effective surface pre-treatment method for recycled rubber particles to improve the sound insulation properties of rubberized lightweight aggregate concrete. Han *et al.* (2018) found that the energy dissipation capacity increases with the increase of the mixed crumb rubber content. The characteristics of acoustic emission sources imply that mixed crumb rubber can effectively improve the crack distribution of crumb rubber concrete. Si *et al.* (2017) investigated the durability of rubberized mortar and concrete samples with NaOH-solution treated rubber particles. The results indicated that the rubberized concrete or mortar (with 15% or 25% NaOH-treated rubber replacement) samples had improved durability.

In addition, the structural performance of members cast with crumb rubber concrete has been studied (Han *et al*. 2015, Ismail and Hassan 2016, Duarte *et al*. 2016, Silva *et al*. 2017, Mendis *et al*. 2018). Yang *et al*. (2019) studied the rubber concrete slabs with steel reinforcement under close-in blast loading. The results showed that the tensile zone damage of rubber concrete slabs was smaller than that of normal concrete slabs under large explosive charges; rubber concrete slabs with steel reinforcements were practical structures for blast resistance, especially when subjected to a large energy detonation. Duarte *et al*. (2018) presented a comparative assessment of rubberized concrete filled square steel tubular columns. The results showed that rubberized concrete filled square steel tubular columns had a marginal higher embodied energy and cost than those of the normal

*Corresponding author, Ph.D.
E-mail: jiongfeng108@126.com

ISSN: 2287-5301 (Print), 2287-531X (Online)

Fig. 1 No. 20 crumb rubber

Table 1 The properties of crumb rubber

Surface color	Bulk density (kg/m^3)	Specific gravity	Moisture content (%)	Fineness modulus (MPa)
black	1060	0.93	1.08	0.85

Table 2 Mix proportion of the recycled crumb rubber concrete

No.	Replacement (%)	No.20 CR (kg·m^{-3})	No.40 CR (kg·m^{-3})	No.80 CR (kg·m^{-3})	C (kg·m^{-3})	FA (kg·m^{-3})	CA (kg·m^{-3})	W (kg·m^{-3})
NC	0	0	0	0	422	531	1257	190
No.20 CR5	5	26.55	0	0	422	504.45	1257	190
No.20 CR10	10	53.10	0	0	422	477.90	1257	190
No.20 CR15	15	79.65	0	0	422	451.35	1257	190
No.40 CR5	5	0	26.55	0	422	504.45	1257	190
No.40 CR10	10	0	53.10	0	422	477.90	1257	190
No.40 CR15	15	0	79.65	0	422	451.35	1257	190
No.80 CR5	5	0	0	26.55	422	504.45	1257	190
No.80 CR10	10	0	0	53.10	422	477.90	1257	190
No.80 CR15	15	0	0	79.65	422	451.35	1257	190

concrete filled square steel tubular column- differences less than 1%. Ismail *et al*. (2017) investigated the strength and cracking characteristics of optimised self-consolidating and vibrated rubberised concrete mixtures with/without steel fibres using large-scale reinforced concrete beams. The results showed that the inclusion of steel fibres could alleviate the reduction in the shear capacity and first cracking moment that resulted from the addition of crumb rubber.Combining crumb rubber and steel fibres contributed to developing sustainable concrete beams with high deformability, reduced self-weight and improved shear capacity. Mendis *et al*. (2017) investigated the flexural behaviour of reinforced beams made of crumb rubber concrete mixes of similar compressive strength

The objectives of this study, are to investigate the effects of crumb rubber size and content on the compressive strength, elastic modulus, peak strain (the strain corresponding to peak stress), shape of the stress-strain curve, and to establish a single equation determining the compressive strength, elastic modulus, the relationship between prism compressive strength, peak strain and the stress-strain relation of crumb rubber concrete.

2. Experimental programme

2.1 Materials

The following materials were used in the concrete: Portland cement (C) type 42.5R, natural fine aggregate (FA) with the particle size of 0-5 mm,fineness modulus of 2.7 and 0.6% moisture content, natural coarse aggregate (CA) with size fraction of 5-20 mm, three different sized crumb rubber (No. 20, No. 40 and No. 80 crumb rubbers). The No. 20 crumb rubber (CR), No. 40 CR and the No. 80 CR were a fine material with size fraction of 0.825 mm, 0.42 mm and 0.18 mm, respectively. Table 1 lists the properties of crumb rubber. The No. 20 crumb rubber is shown in Fig. 1.

2.2 Mix proportions

The concrete mixture is based on the specifications for mix proportion designs of ordinary concrete (JGJ55-2011 2011). The CRC mixtures are designed having a constant water/cement ratio of 0.45. The fine aggregates are replaced with different graded crumb rubbers (No. 20, No. 40, No. 80 crumb rubber) respectively, at four designated contents of 0%,5%,10%,15% by mass. The coarse aggregate, cement and water of CRC are present in quantities equal to those in the NC. Totally ten different CRC mixtures are designed. Table 2 provides the design of the concrete mix.

2.3 Specimen preparation

The preparation and curing of all mixes were conducted in the State Key Laboratory for Concrete Material Research at East China Institute of Technology in Nanchang, China. Three cubic specimens per each mix of 150×150×150 mm are prepared for cubic compressive strength of each level of crumb rubber content. In total, 30 cubic compressive strength tests are completed by using the cubic specimens. Six prism specimens per each mix of 150×150×300 mm are prepared for stress-strain of each level of crumb rubber content. In total, 60 tests are completed by using the prism specimens. For each mix at each laboratory conditions. The dry cement and aggregates were mixed for 1 minute in a 0.05 m^3 laboratory mixer. The mixing continued for the next minute, with about 70% of water added. The mixing continued for another 1 minute. After casting, the concrete specimens were kept in their moulds for 24h at room temperature (20±2°C). After 24h, the specimens were demoulded and cured in a room with 20±2°C, and 95% relative humidity for 28 days.

2.4 Testing

The compressive behavior of concrete specimen for

Fig. 2 Test setup

each mix proportion was tested according to JGT/T70-2009. The loading setup was a YAW-3000 microcomputer controlled electro-hydraulic servo tester, as shown in Fig. 2. In order to obtain the complete stress-strain curves, the deformation rate of the test specimens was kept constant at 0.3 mm/min. During the experiment, the axial compression and vertical deformation values of test specimens were automatically collected by the computer installed. Cubic compressive strength is obtained from the test. To obtain the strain values, two Linear Variable Displacement Transducers (LVDTs) were used to measure the displacement on the prism specimens. The prism compressive strength, corresponding to peak stress, is obtained directly from stress-strain curves. The modulus of elasticity (E_c) is calculated according to prism stress and prism strain, as follows

$$E_c = \frac{\sigma_{c2} - \sigma_{c1}}{\varepsilon_2 - 0.00005} \tag{1}$$

in which σ_{c2} is the stress corresponding to 40% of the peak stress, σ_{c1} is the stress corresponding to a strain of 0.00005, and ε_2 is the strain at the stress level σ_{c2}.

3. Results and discussion

3.1 Failure behaviour

Fig. 3 shows the failure pattern of concrete specimens. As shown, when ordinary concrete is subjected to uniaxial compression failure, the cracks appear along the diagonal direction of the specimen, and then the splitting crack with a large width penetrates the whole specimen. The specimens are accompanied by some spalling and the specimen shape is changed due to the relative slip of the inclined shear failure interface. The failure pattern of NC belongs to the typical shear brittle failure. Compared with ordinary concrete, the failure cracks of crumb rubber concrete have obvious changes. The macro-failure cracks of crumb rubber concrete are basically parallel to the direction of axial pressure, and there is no phenomenon of failure crack penetration. The width and length of cracks are relatively small, the distribution of cracks is relatively

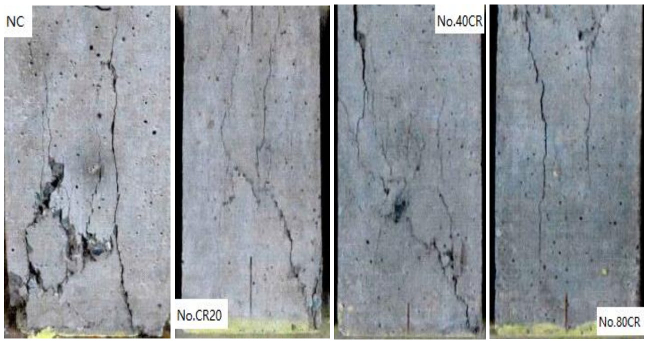

Fig. 3 Failure pattern of concrete prism

Table 3 Experiment results of the specimens

Specimen	Rubber content (%)	f_{cu} (MPa)	f_c (MPa)	E_c (GPa)
NC	0	38.3	26.4	26.9
No.20 CR5	5	34.4	23.9	25.1
No.20 CR10	10	30.4	21.1	22.6
No.20 CR15	15	27.8	19.1	20.9
No.40 CR5	5	34.1	23.4	24.6
No.40 CR10	10	30.2	20.7	22.2
No.40 CR15	15	27.3	18.6	20.4
No.80 CR5	5	33.9	23.1	24.1
No.80 CR10	10	30.1	20.1	21.5
No.80 CR15	15	26.7	18.1	19.9

Notes: f_{cu} is cube compressive strength, f_c is prism compressive strength.

dispersed and the probability of intersection between cracks is low. Crumb rubber concrete under uniaxial compression has good integrity, no obvious spalling phenomenon, and the specimen shape has not changed, that is, the relative slip of the failure interface inside the concrete is very small. That is to say, the failure pattern of CRC belongs to the columnar compression failure.

3.2 Compressive strength

Table 3 gives the average values of experiment results. As can be seen from Table 3, Fig. 4, the cube compressive strength of concrete decrease with an increase in crumb rubber content. For example, the cube compressive strength of No .20 crumb rubber specimen with rubber contents of 5%, 10%, 15% decreases by about 10.2%, 20.6%, 27.4%. This is probably due to the weaker bond between the rubber and the matrix. In addition, the cube compressive strength of concrete decrease as the crumb rubber size decreases. The cube compressive strength at 10% of No. 20, No. 40, No. 80 crumb rubber specimen are 30.4 MPa, 30.2 MPa and 30.1 MPa, respectively. Based on the test results, Eq. (2) is proposed to determine the cube compressive strength of CRC

$$f_{cu,cr} = f_{cu} \cdot e^{\frac{-2.175r \cdot d}{d - 0.0169}} \tag{2}$$

in which $f_{cu,cr}$, f_{cu} is the cube compressive strength of CRC and NC, respectively; r is the crumb rubber content, and d is the crumb rubber size. Fig. 5 shows a comparison between the calculated results using Eq. (2) and the

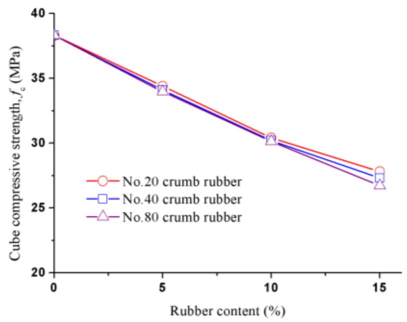

Fig. 4 Cube compressive strength of CRC

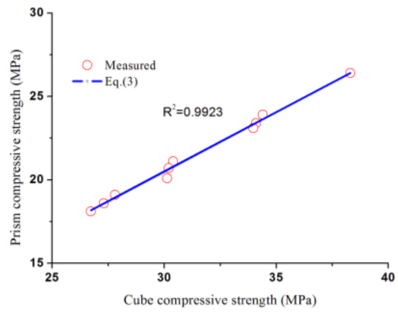

Fig. 7 The relationship between prism compressive strength and cube compressive strength

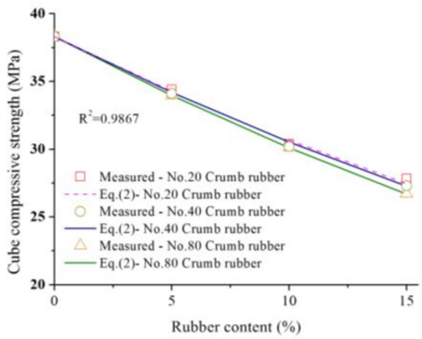

Fig. 5 Comparison between calculated and measured cube compressive strength

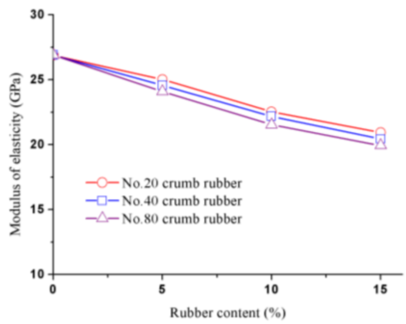

Fig. 8 Modulus of elasticity for CRC

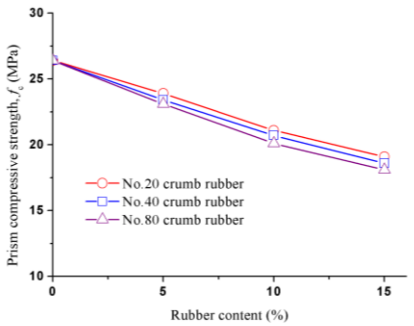

Fig. 6 Prism compressive strength of CRC

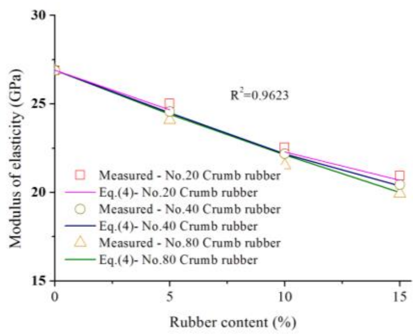

Fig. 9 Comparison between calculated and measured modulus of elasticity

measured results of cube compressive strength. It can be seen that the calculated results agree well with the measured results, implying that Eq. (2) being applied to the crumb rubber concrete.

It can be seen from Table 3 and Fig. 6, the prism compressive strength is the same as cube compressive strength that it decreases as the crumb rubber content increase or the crumb rubber size decrease. And according to the measured results, the relationship between prism compressive strength and cube compressive strength can be proposed as follows

$$f_{c,\mathrm{cr}} = 0.712 f_{cu,cr} \text{-} 0.848 \tag{3}$$

in which $f_{cu,\mathrm{cr}}$, $f_{c,cr}$ is the cube compressive strength and prism compressive strength of CRC, respectively. The relationship between prism compressive strength and cube compressive strength is shown in Fig. 7. It can be seen that the calculated results using Eq. (3) are generally in good agreement with the measured results.

3.3 Elastic modulus in compression

Fig. 8 shows modulus of elasticity of all concrete specimens. As shown, the modulus of elasticity of CRC is less than that of NC. The modulus of elasticity decreases with the increase in crumb rubber content at a given crumb rubber size. For example, the modulus of elasticity of No.40 crumb rubber specimen with rubber contents of 5%, 10%, 15% decreases by about 8.6%, 17.5%, 24.0%. And for a given crumb rubber content, the modulus of elasticity of CRC increases slightly as the crumb rubber size increases. The modulus of elasticity at 15% of No. 80, No. 40, No. 20 crumb rubber specimen increases by about 25.9%, 24.0%, 22.1%, respectively.

Based on the test results, Eq. (4) is proposed to determine the modulus of elasticity for CRC

$$E_{\mathrm{cr}} = \frac{10^2}{0.759 + \dfrac{113.315}{f_{cu,cr}}} \tag{4}$$

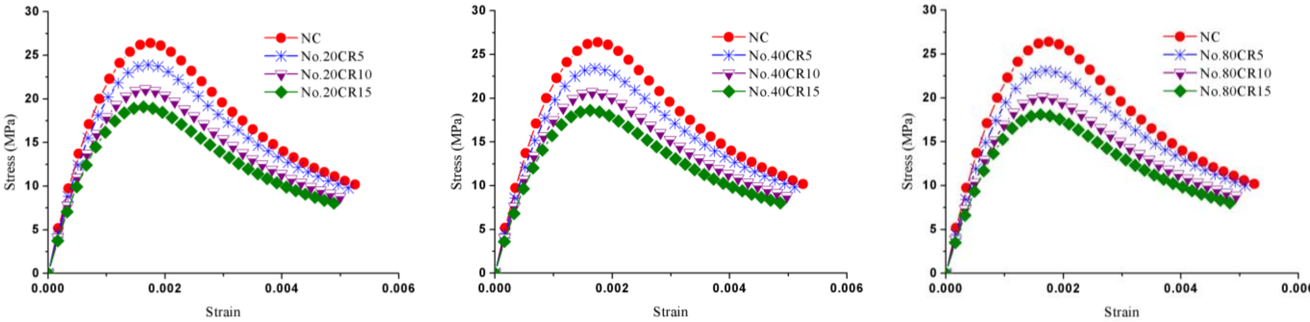

(a) No. 20CR with respect to NC (b) No. 40CR with respect to NC (c) No. 80CR with respect to NC

Fig. 10 Typical stress-strain curves of crumb rubber concrete

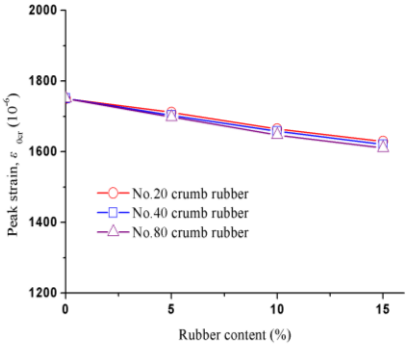

Fig. 11 Peak strain of CRC

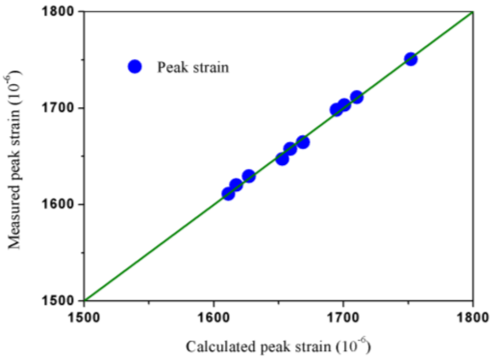

Fig. 12 Comparison between calculated and measured peak strain

in which E_{cr}, is the modulus of elasticity of CRC; $f_{cu,cr}$ is the cube compressive strength of CRC. Fig. 9 shows a comparison between the calculated results using Eq. (4) and the measured results of modulus of elasticity. It can be seen that the calculated results agree well with the measured results.

3.4 Stress-strain curves

Fig. 10 shows the complete stress-strain curves of CRC with different crumb rubber content. As noted, the shape of the ascending branch of the stress-strain curves for all concrete specimens present very similar regardless of the crumb rubber size and content. The shape is linear up to about 35% of the maximum stress and then it becomes parabolic. And it is worth mentioning that by adding crumb rubber increases the strain of the concrete under the same unit stress, and the higher the crumb rubber content is, the higher the strain will be; the lower the crumb rubber size is, the higher the strain will be. The reason may be the lower elastic modulus of the crumb rubber. And as previously described in this study, the modulus of elasticity decreases with the increasing of crumb rubber content. The shape of the descending branch of the stress-strain curves for all concrete specimens is also similar. However, the slope of descending branch increases as the crumb rubber content increases. Hence, this increase implies a decrease in the ultimate strain and an increase in the ductility of concrete.

3.5 Peak strain and ultimate strain

Fig. 11 shows the peak strain (at the maximum stress) of all concrete specimens. The peak strain of crumb rubber concrete is less than that of natural concrete. For example, the peak strain values of NC, No. 20CR5, No. 20CR10 and No. 20CR15 are 0.00175, 0.00171, 0.00166 and 0.00162, respectively. And with the increasing of the crumb rubber content, the values of peak strain decrease. For specimen No.40CR15 with a rubber content r=15%, the peak strain is decreased by about 7.45%. Fig. 11 also reveals that the crumb rubber size has some effect on the peak strain. The peak strains of concrete specimens increase with increasing crumb rubber size. Based on the test results, the following formula is proposed to determine the peak strain for the crumb rubber concrete as

$$\varepsilon_{\text{ocr}} = 337.09\sqrt{f_c} \times (1 - 0.481r + 0.014d) \tag{5}$$

Where ε_{ocr} is the peak strain of CRC, f_c is the prism compressive strength of NC, r is the crumb rubber content, and d is the crumb rubber size.

Fig. 12 shows a comparison between the calculated results using Eq. (4) and the measured results. It can be seen from Fig. 12 that the calculated results using Eq. (4) are generally in good agreement with the measured results for the specimens in this study.

Fig. 13 shows the ultimate strain (at a stress level equals to 85% of the maximum stress) of all concrete specimens. It reveals that the ultimate strain decreases with increasing crumb rubber content. And it increases with increasing crumb rubber size. Fig. 14 shows the influence of the crumb rubber content on the $\varepsilon_{ucr}/\varepsilon_{ocr}$ value of CRC. It can be seen that the $\varepsilon_{ucr}/\varepsilon_{ocr}$ value of CRC is larger than that

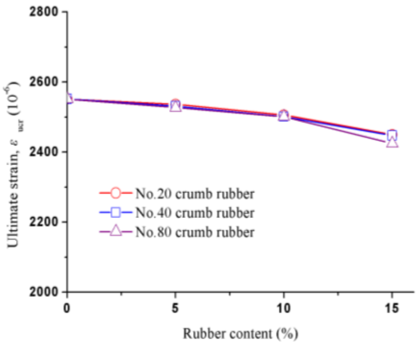

Fig. 13 Ultimate strain of CRC

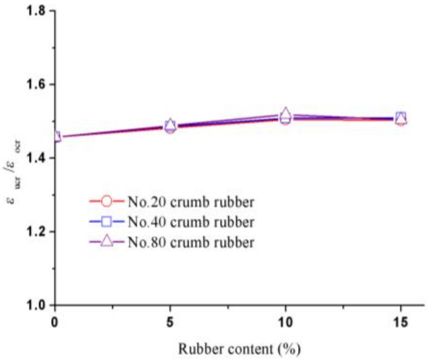

Fig. 14 Dependence of $\varepsilon_{ucr}/\varepsilon_{ocr}$ on rubber content

of the normal concrete. This means that the CRC is less brittle with good ductility than that of the normal concrete.

3.6 Modeling the stress-strain relationship

In structural application of crumb rubber concrete, a model equation of the stress-strain curve for crumb rubber concrete is desirable and necessary for the structural analysis and design. As shown in section 3.4, the crumb rubber content and size have some influence on the shape of the stress-strain curve. Hence, in this study, a stress-strain model for CRC is proposed according to the test results and the analytical expression suggested by Guo and Zhang (1982) with some parameters redefined. Specifically, the normalized stress-strain relation is approximated by the following equation

$$y = \begin{cases} ax + (3-2a)x^2 + (a-2)x^3, 0 \le x < 1 \\ \dfrac{x}{b(x-1)^2 + x}, x \ge 1 \end{cases} \tag{6}$$

where~~,~~ $x=\varepsilon/\varepsilon_{0cr}$, $y=\sigma/f_{c,cr}$, a and b are the constants to defining the ascending and descending curves, respectively. Based on the experimentally obtained stress-strain curves of CRC, parameters a and b are obtained by a regression analysis. The results are given as follows

$$\begin{aligned} a &= e^{(0.0116 r \cdot d + 0.0109\ln(d+0.0645)+0.7266)} \\ b &= e^{(-1.2103 r \cdot d + 0.2734\ln(d+0.5204)+0.0792)} \end{aligned} \tag{7}$$

As shown in Fig. 15, the using of the analytical expressions is in good agreement with experimental results implying that they can be applied to crumb rubber concrete. More studies are, however, needed to further validate the model for this concrete material.

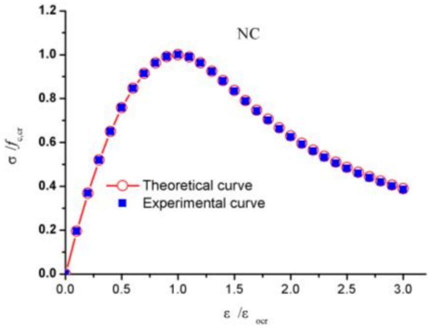

(a) NC

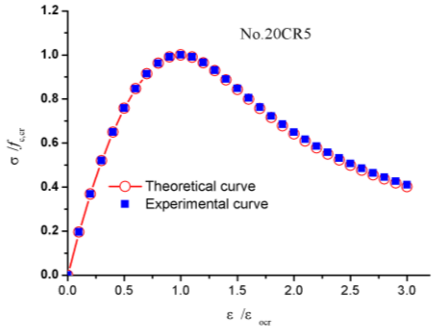

(b) No. 20CR5

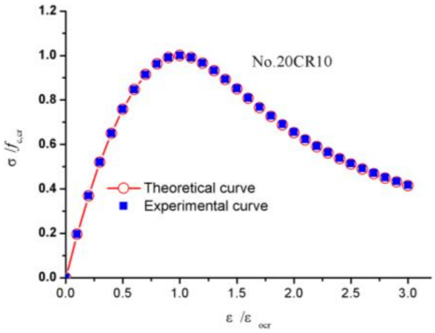

(c) No. 20CR10

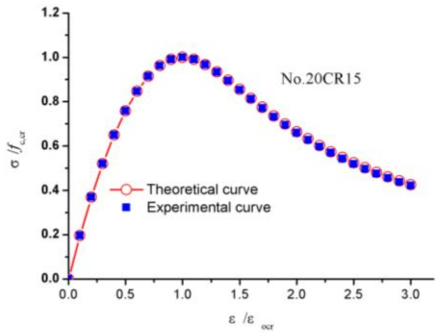

(d) No. 20CR15

Fig. 15 Comparison of the normalized stress-strain curves

4. Conclusions

Based on the results obtained from the experimental results, the following conclusions can be drawn:

(1) The typical failure mode of crumb rubber concrete is columnar compression failure. And the incorporation of crumb rubber in concrete either delays the failure of the concrete specimens or reduces of the degree of failure.
(2) The compressive strength including the cube and prism compressive strength of CRC decrease with increase in crumb rubber content or with decrease in crumb rubber size. The cube compressive strength of CRC calculated by using the proposed equation Eq. (1) generally agrees well with the test results. The relationship between prism compressive strength and cube compressive strength of CRC calculated by using the proposed equation Eq. (2) is generally in good agreement with the measured results.
(3) The modulus of elasticity of CRC decreases with the increasing crumb rubber content or with the decreasing in crumb rubber size in a fashion similar to that observed in compressive strength. Eq. (3) is proposed to determine the modulus of elasticity of CRC, and the calculated results are in good agreement with the measured results.
(4) The crumb rubber size and content have some effect on the stress-strains of CRC. With the increasing of the crumb rubber content or the decreasing crumb rubber size, the peak strain decreases. The proposed equation Eq. (4) is well fit with the test results.
(5) The proposed equation of stress-strain curve for crumb rubber concrete is in good agreement with experimental results implying that they can be applied to crumb rubber concrete.

Acknowledgments

The authors are grateful to the financial support provided by the Chinese National Natural Science Foundation (No. 51868001,51608435), the Natural Science Foundation of Jiangxi Province (No. 20171BAB206053), the Technology Support Project of Jiangxi Province (No. 20161BBH80045), and the Opening Fund of State Key Laboratory of Green Building in Western China (Grant No.lskf201903).

References

Bharathi Murugan, R. and Natarajan, C. (2017), "Investigation on the use of waste tyre crumb rubber in concrete paving blocks", *Comput. Concrete*, **20**(3), 311-318. https://doi.org/10.12989/cac.2017.20.3.311.

Duarte, A.P.C., Silva, B.A., Silvestre, N., de Brito, J., Julio, E. and Castro, J.M. (2016), "Finite element modelling of short steel tubes filled with rubberized concrete", *Compos. Struct.*, **150**, 28-40. https://doi.org/10.1016/j.compstruct.2016.04.048.

Duarte, A.P.C., Silvestre, N., de Brito, J., Julio, E. and Silvestre, J.D. (2018), "On the sustainability of rubberized concrete filled square steel tubular columns", *J. Clean. Prod.*, **170**, 510-521. https://doi.org/10.1016/j.jclepro.2017.09.131.

Emiroglu, M., Yildiz, S. and Kelestemur, M.H. (2015), "A study on dynamic modulus of self-consolidating rubberized concrete", *Comput. Concrete*, **15**(5), 795-805. https://doi.org/10.12989/cac.2015.15.5.795.

Fu, C., Ye, H., Wang, K., Zhu, K. and He, C. (2019), "Evolution of mechanical properties of steel fiber-reinforced rubberized concrete (FR-RC)", *Compos. Part B-Eng.*, **160**, 158-166. https://doi.org/10.1016/j.compositesb.2018.10.045.

Guo, Z.H. and Zhang, X.Q. (1982), "Experimental investigation of stress-strain curves for concrete", *Chin. J. Build. Struct.*, **3**(1), 1-12. (in Chinese)

Gupta, T., Tiwari, A., Siddique, S., Sharma, R.K. and Chaudhary, S. (2017), "Response assessment under dynamic loading and microstructural investigations of rubberized concrete", *J. Mater. Civil Eng.*, **29**(8), 19-23. https://doi.org/10.1061/(ASCE)MT.1943-5533.0001905.

Han, Q.H., Xu, J., Xing, Y. and Li, Z.L. (2015), "Static push-out test on steel and recycled tire rubber-filled concrete composite beams", *Steel Compos. Struct.*, **19**(4), 843-860. https://doi.org/10.12989/scs.2015.19.4.843.

Han, Q.H., Yang, G. and Xu, J. (2018), "Experimental study on the relationship between acoustic emission energy and fracture energy of crumb rubber concrete", *Struct. Control Hlth.*, **25**(10), 1-9. https://doi.org/10.1002/stc.2240.

Ismail, M.K. and Hassan, A.A.A (2016), "Performance of full-scale self-consolidating rubberized concrete beams in flexure", *ACI Mater. J.*, **113**(2), 207-218.

Ismail, M.K., Hassan, A.A.A. and Hussein, A.A. (2017), "Structural behaviour of reinforced concrete beams containing crumb rubber and steel fibres", *Mag. Concrete Res.*, **69**(18), 939-953. https://doi.org/10.1680/jmacr.16.00525.

Mendis, A.S.M., Al-Deen, S. and Ashraf, M. (2017), "Effect of rubber particles on the flexural behaviour of reinforced crumbed rubber concrete beams", *Constr. Build. Mater.*, **154**, 644-657. https://doi.org/10.1016/j.conbuildmat.2017.07.220.

Mendis, A.S.M., Al-Deen, S. and Ashraf, M. (2018), "Flexural shear behaviour of reinforced crumbed rubber concrete beam", *Constr. Build. Mater.*, **166**, 779-791. https://doi.org/10.1016/j.conbuildmat.2018.01.150.

Padhi, S. and Panda, K.C. (2016), "Fresh and hardened properties of rubberized concrete using fine rubber and silpozz", *Adv. Concrete Constr.*, **4**(1), 49-69. https://doi.org/10.12989/acc.2016.4.1.049.

Ramdani, S., Guettala, A., Benmalek, M.L. and Aguiar, J.B. (2019), "Physical and mechanical performance of concrete made with waste rubber aggregate, glass powder and silica sand powder", *J. Build. Eng.*, **21**, 302-311. https://doi.org/10.1016/j.jobe.2018.11.003.

Si, R.Z., Guo, S.C. and Dai, Q.L. (2017), "Durability performance of rubberized mortar and concrete with NaOH-Solution treated rubber particles", *Constr. Build. Mater.*, **153**, 496-505. https://doi.org/10.1016/j.conbuildmat.2017.07.085.

Silva, A., Jiang, Y., Castro, J.M., Silvestre, N. and Monteiro, R. (2017), "Monotonic and cyclic flexural behaviour of square/rectangular rubberized concrete-filled steel tubes", *J. Constr. Steel Res.*, **139**, 385-396. https://doi.org/10.1016/j.jcsr.2017.09.006.

Specification for Mix Proportion Design of Ordinary Concrete (JGJ55-2011), Chinese Building Construction Publishing Press, Beijing. (in Chinese)

Standard for Test Method of Basic Properties of Construction Moatar in China (JGT/T70-2009), Chinese Building Construction Publishing Press, Beijing. (in Chinese)

Thomas, B.S., Gupta, R.C., Mehra, P. and Kumar, S. (2015), "Performance of high strength rubberized concrete in aggressive environment", *Constr. Build. Mater.*, **83**, 320-326. https://doi.org/10.1016/j.conbuildmat.2015.03.012.

Williams, K.C. and Partheeban, P. (2018), "An experimental and numerical approach in strength prediction of reclaimed rubber concrete", *Adv. Concrete Constr.*, **6**(1), 87-102. https://doi.org/10.12989/acc.2018.6.1.087.

Yang, F., Feng, W., Liu, F., Jing, L., Yuan, B. and Chen, D. (2019), “Experimental and numerical study of rubber concrete slabs with steel reinforcement under close-in blast loading”, *Constr. Build. Mater.*, **198**, 423-436. https://doi.org/10.1016/j.conbuildmat.2018.11.248.
Yang, F., Feng, W., Liu, F., Jing, L., Yuan, B. and Chen, D. (2019), “Experimental and numerical study of rubber concrete slabs with steel reinforcement under close-in blast loading”, *Constr. Build. Mater.*, **198**, 423-436. https://doi.org/10.1016/j.conbuildmat.2018.11.248.
Zhang, B.Y. and Poon, C.S. (2018), “Sound insulation properties of rubberized lightweight aggregate concrete”, *J. Clean. Prod.*, **172**, 3176-3185. https://doi.org/10.1016/j.jclepro.2017.11.044.

CC